3-8-2013

Nanoparticle Film Assemblies as Platforms for Electrochemical Biosensing – Factors Affecting Amperometric Signal Enhancement of Hydrogen Peroxide

Adrienne R. Schmidt

Natalie D. T. Nguyen

Michael C. Leopold
University of Richmond, mleopold@richmond.edu

Recommended Citation

For submission to Langmuir

Nanoparticle Film Assemblies as Platforms for Electrochemical Biosensing – Factors Affecting Amperometric Signal Enhancement of Hydrogen Peroxide

Adrienne R. Schmidt, Natalie D.T. Nguyen, and Michael C. Leopold*

Department of Chemistry, Gottwald Center for the Sciences, University of Richmond Richmond, VA 23173

Abstract

Factors affecting the enhanced amperometric signal observed at electrodes modified with polyelectrolyte-gold nanoparticle (Au-NP) composite films, potential interfaces for first generation biosensors, were systematically investigated and optimized for hydrogen peroxide (H_2O_2) detection. Polyelectrolyte multilayer films embedded with citrate-stabilized gold nanoparticles exhibited high sensitivity toward the oxidation of H_2O_2. From this Au-NP film assembly, the importance of Au-NP ligand protection, film permeability, density of Au-NPs within the film, as well as electronic coupling between Au-NPs (inter-particle) and between the film and the electrode (interfacial) were evaluated. Using alternative Au-NPs, including those stabilized with thiols, polymers, and bulky ligands suggests that amperometric enhancement of H_2O_2 is optimized at poly-L-lysine linked film assemblies embedded with Au-NPs possessing small, charged, and conductive (conjugated) peripheral ligands. As a potential application of these Au-NP film assemblies, an enhanced amperometric signal for H_2O_2 oxidation was shown for modified "needle" electrodes. The overall aim of this research is to gain greater understanding of designing electrochemical sensing strategies that incorporate Au-NPs and target specific analytes.

Keywords:

*To whom correspondence should be addressed. Email: mleopold@richmond.edu.
Phone: (804) 287-6329. Fax: (804) 287-1897

Introduction

The development of new materials and methods for advancing biosensor technology continues to be a major focus of research activity aiming to ultimately produce *in-vivo* sensors for clinically relevant physiological targets. The ability to create biocompatible and functional devices for the real-time, continuous monitoring of a specific biological analyte, however, remains a complex challenge from both fundamental analytical measurement and materials science standpoints.[1,2] A standard set of criteria applies to evaluating any chemical sensor's performance including its selectivity, adequate sensitivity, rapid response for real time monitoring, and the propensity to be microfabricated in a biocompatible manner for eventual implantation and *in-vivo* operation. Amperometric electrochemical biosensing is a prominent area of study within this field as, in theory and in practice, it can accommodate a number of important factors, including relatively simple signal mechanisms, fast response times, and inexpensive instrumentation/materials/operation that can be readily miniaturized.[3]

First generation electrochemical biosensors, a popular strategy for amperometric-based sensing,[3] signal the presence of a target analyte via the oxidation of hydrogen peroxide (H_2O_2), a natural byproduct of the highly selective reaction between the analyte and its corresponding enzyme normally harnessed within the biosensor design. The use of the enzyme glucose oxidase (GOx) immobilized at an electrode interface, for example, provides selectivity for a reaction with glucose that produces H_2O_2 that is subsequently oxidized at a working electrode to produce an amperometric signal.[3] Two critical issues with the development of functional first generation biosensing schemes are (1) the successful immobilization of multi-layers of active, stable enzymes at the electrode and (2) the construction of an electrode interface or platform that provides adequate sensitivity (i.e., high signal-to-noise ratios) toward the electrochemical

2

detection of H_2O_2. For the former issue, researchers have explored strategies that incorporate multi-layers of immobilized enzymes within a 3-dimensional network at electrodes including electropolymerization,[4-6] nanoporous gold,[7] and sol-gel chemistry.[8-10] The latter challenge, and the focus of the work herein, revolves around the establishment of an electrode interface with efficient electrical communication between the biological recognition event (chemical signal) and transducer (WE), a relationship that is often challenged by the protein/enzyme's insulating shell of amino acids and/or the required synthetic modification of the electrode (e.g., self-assembled monolayers, SAMs) designed to preserve the native structure/function of the incorporated enzymes.[3]

One of the more notable strategies employed to improve the efficiency of amperometric biosensors over the past several years has been the incorporation of nanomaterials (NMs) at or near the electrochemical interface. Indeed, several reviews explore NMs used in this capacity, ranging from metallic and semiconductor nanoparticles (NPs) to carbon-based NMs (e.g., nanotubes).[11-14] More specific literature reviews with a sharper focus on metallic NPs and their incorporation into sensor designs are also available,[15-17] including several more recent studies that utilize colloidal gold NPs (Au-NPs) as functional components of biosensing schemes.[17-19] The work done in these research reports reflects an effort to capitalize on the novel properties of the Au-NPs as a means of enhancing sensitivity by creating a sensing platform that acts as a highly efficient electrochemical interface while maintaining the biomolecule's structure/function. Indeed, the direct coupling of proteins/enzymes to Au-NPs is a well-known phenomenon; literature reports by Crumbliss,[20] Niemeyer,[21] and Rotello[22] highlight several key advantages of interfacing proteins with colloidal Au-NPs, including large surface-to-volume ratios for a high density of adsorbed, native-structure and functional biomolecules. Additionally, Au-NP film

assemblies allow for readily manipulated surface chemistry and the metallic cores can act as conduits for facilitating critical electrochemical reactions.

Within the body of work studying Au-NP based platforms, different linking systems interconnecting the Au-NPs at electrode interfaces have been explored. Polyelectrolytes have been employed in this capacity by Murray, Fermin, and our lab, to create composite films featuring carboxylic functionalized monolayer protected clusters (MPCs)[23] as well as several types of water-soluble Au-NPs.[24-29] Some of these films, including those from our own experiments, were shown to yield enhanced voltammetric signals of simple solution redox species.[25, 26] More recent studies suggest that the incorporation of Au-NPs into film assemblies consistently results in more sensitive amperometric detection of targeted analytes.[30-33] Several reports[34,35] focus exclusively on developing Au-NP-film interfaces or biosensor platforms, several utilizing polymer-linked Au-NP films, specifically target more sensitive electrochemical detection of H_2O_2.[36-38] However, in spite of the number of reports examining electrochemical interfaces incorporating Au-NPs within polymeric matrices, few of them delve into the fundamental mechanism/understanding and control or optimization of the observed electrochemistry that is attributed to the use of Au-NPs within their strategies. Given this level of understanding, the development of highly sensitive, optimized Au-NP-based electrochemical interfaces coupled with a greater fundamental understanding of its structure-function relationships remains a study of significant value to the field.

In this report, we develop films of polyelectrolyte multi-layers (PEMs) with embedded Au-NPs as an electrochemical interface that provides significant enhancement in sensitivity toward the amperometric detection of H_2O_2 oxidation as it would relate to first generation biosensing. Previous studies conducted in our laboratory have focused on the assembly and

stability of Au-NP films of this nature.[28,29] More recent work in our lab, and by others, has established that electrodes modified with PEM films incorporating citrate-stabilized Au-NPs (CS-NPs) result in enhanced currents in the cyclic voltammetry of freely diffusing redox species like potassium ferricyanide, even at completely blocked electrodes exhibiting no prior Faradaic current.[25-27] Expanding on this observation and recognizing its direct relevance for first generation biosensor development, our current study focuses on creating interfacial platforms involving Au-NP film assemblies that are able to significantly enhance the amperometric detection of H_2O_2. As part of our study, we explore various aspects of the films that influence the observed amperometric signal enhancement, including the Au-NP density, electronic coupling, and mass transport of H_2O_2 through the film, as well as the importance of Au-NP core size and stabilizing ligands. Au-NP film modifications to needle/wire electrodes showed significant amplification of amperometric signals as well.

Experimental Details

Materials, Equipment, and Instrumentation

All chemicals were purchased commercially (Sigma-Aldrich) and used as received unless otherwise stated. All glassware was cleaned with aqua regia (3:1, HCl/HNO_3) and rinsed with 18 $M\Omega$ ultra-pure (UP) H_2O prior to use. Cyclic voltammetry and amperometric current-time (*I-t*) experiments were performed using either a CH Instruments' potentiostat (Model 650A) or an 8-channel multi-potentiostat (Model 1000B). Unless otherwise stated, electrochemical measurements were made in solutions of 4.4 mM potassium phosphate buffer (KPB) at pH= 7 vs. Ag/AgCl (satr. KCl) reference electrode (CH Instruments) at gold electrodes (CH Instruments). Perfluoroalkoxy (PFA) polymer-coated gold wire (0.003" bare diameter; 0.0055"

coated diameter) was purchased (A-M Systems) and used as "needle" or wire electrodes where the PFA is mechanically stripped to create the working electrode (~ 1 cm) and electrical contact (Supporting Information), subsequently cleaned by voltammetric cycling in 0.1 M H_2SO_4. Ultraviolet and visible spectroscopy (UV-Vis) was performed on an Agilent 8453 photodiode array spectrophotometer. A JEOL 1010 transmission electron microscope (TEM) was used for nanoparticle characterization at 80-100 kV. Aqueous Au-NP solutions were drop casted on 400 mesh Formvar-covered copper grids (Electron Microscopy Sciences) and wicked off several minutes later prior to imaging.

Synthesis of citrate-stabilized gold nanoparticles (CS-NPs)

Citrate-stabilized gold nanoparticles (CS-NPs) were created according to previously reported methods.[27,39] Briefly, a 1 mM $HAuCl_4$ (100 mL) aqueous solution was heated to reflux while being stirred. Immediately after the solution reached reflux, a 38.8 mM sodium citrate (10 mL, aq) solution was rapidly added, causing the solution to undergo immediate color transitions from pale yellow to colorless to purple to wine red. The solution was heated for 10 additional minutes and then allowed to cool to room temperature while being continuously stirred. The solution was filtered with a 0.8 μm Gelman membrane filter and stored in the dark until further use. CS-NPs were characterized with UV-Vis spectroscopy and TEM imaging (see Supporting Information). The average core diameter for CS-NPs is reported as 10.3 ± 2.7 nm.[27]

Nanoparticle Film Assembly Procedure

Polyelectrolyte films embedded with Au-NPs were constructed according to previously reported procedures from our group as well as other laboratories.[23-25, 40] Typically, gold button electrodes

6

(CH Instruments) were polished with successively smaller alumina powder (1 μm, 0.3 μm, 0.05 μm) water mixtures on a polishing wheel before being electrochemically cycled in 0.1 M H_2SO_4 to achieve repeatable, expected voltammetry for a clean gold surface.[26]   Freshly cleaned electrodes were immediately modified with a self-assembled monolayer (SAM) via a > 24 hour exposure to 5 mM ω-substituted alkanethiols in ethanol (e.g., 11-mercaptoundecanoic acid (MUA), 6-mercaptohexanoic acid (MHA), or 16-mercaptohexadecanoic acid (MHDA)). SAM-modified electrodes were then copiously rinsed with ethanol and UP H_2O prior to further use. For film assembly, as previously reported, the SAM-modified electrodes were exposed to alternating solutions of 1 mg/mL poly-L-lysine (PLL) and Au-NPs solution for 15 minutes and 1 hour, respectively. Between solutions, the electrodes were rinsed copiously with UP H_2O. As in previous reports,[41] film growth was again monitored electrochemically using cyclic voltammetry to measure the double layer capacitance or charging current in KPB and then indirectly confirmed with spectroscopic measurements of analogous films assembled on glass slides silanized with 3-(aminopropyl)trimethoxysilane (3-APTMS) after each exposure to Au-NPs (Supporting Information).

Synthetic Procedures for Alternative Nanoparticles

Procedures and characterization for synthesizing alternative nanoparticles, including MUA-exchanged hexane thiol, thioctic acid (TA), 3-mercaptopropionic acid (MPA), polyvinylpyrrolidone (PVP), 4-mercaptobenzoic acid (MBA) and cholate (CHO) stabilized NPs, were conducted as in prior literature reports[27-29,41-49] and are detailed in the Supporting Information.

Results and Discussion

Assembly, Characterization, and Performance of PEM CS-NP Modified Electrodes

The basis for our initial electrode modifications to optimize amperometric detection of H_2O_2 was prior work from our lab and others showing that poly-electrolyte multi-layer (PEM) films embedded with citrate-stabilized gold nanoparticles (CS-NPs) resulted in voltammetry of solution species with notably faster electron transfer (ET) kinetics.[26] Within that study, the most successful film geometry was identified to be a SAM-modified electrode subsequently exposed to alternating solutions of poly-L-lysine (PLL) as a linking system between CS-NPs. This type of film geometry is depicted in Scheme I and represents the starting point for the current study that focuses on optimizing amperometric responses for H_2O_2 oxidation at Au-NP films.

As in prior reports,[26-28, 41] the progressive growth of NP film assemblies in this geometry (**Scheme I**) and composed of these materials (i.e., gold electrode and polyelectrolytes at SAM modified electrodes) can be monitored electrochemically by measuring increasing charging current or double-layer capacitance that results from increasing incorporation of Au-NPs into the film. Analogous films assembled on glass can be monitored by the increasing strength of absorbance of the surface plasmon band associated with Au-NPs. Examples of these film growth monitoring techniques are shown in **Figure 1**. Additionally, traditional electrochemical probing, where the voltammetry of potassium ferricyanide ($Fe(CN)_6^{3-/4-}$) is observed at each step of the PEM-NP film assembly, progresses as expected during film formation. That is, $Fe(CN)_6^{3-/4-}$ is completely blocked from the electrode after MUA SAM modification and initial PLL exposure, but a resurgent voltammetric signal from the probe is observed with the addition of Au-NPs, a signal that then displays increasing voltammetric peak separation with additional exposures to PLL and Au-NPs (see Supporting Information). These techniques for verifying PEM-NP film

growth were consistent regardless of the type of Au-NPs used in the study (see Supporting Information).

In designing an electrochemical platform incorporating Au-NPs at the interface for the optimal detection of H_2O_2, a typical experiment involves running amperometric *I-t* tests where the electrode is held at a potential to oxidize H_2O_2 (+0.65 V) and aliquots of H_2O_2 are periodically injected in order to assess the sensitivity of the electrode interface, the Au-NP film platform. **Figure 2** shows representative *I-t* curves for this type of experiment where injections of H_2O_2 correspond to 0.1 mM increases in H_2O_2 concentration in stirred bulk solution. As seen in the results, H_2O_2 injections at a MUA SAM-modified electrode (Figure 2, inset) result in a very small amperometric response whereas the same injections at a poly-L-lysine (PLL) linked CS-NP film results in a significantly enhanced signal. For example, the first injection (i.e., the first step) yielding, resulting in 0.1 mM H_2O_2 bulk solution, yields an anodic current (~2.4 µA) for the oxidation of H_2O_2 that is two orders of magnitude or 35x greater than the same injection at a MUA-SAM modified electrode (~0.068 µA). This observed enhancement, a highly repeatable relative result, occurs at the PLL-linked CS-NP film assemblies in spite of the fact that the base of such films, a MUA SAM (Scheme I), remains intact. Similar "enhancements" of H_2O_2 oxidation current were observed at PLL-linked CS-NP film formed at electrodes modified with both longer 16-mercaptohexadecanoic acid and shorter 6-mercaptohexanoic acid SAMs as well (see Supporting Information).

The observed enhancement of the H_2O_2 signal is exclusively attributed to the embedded CS-NPs within the film assembly. A control experiment where anionic poly(4-styrene) sulfonate (PSS) is substituted for the anionic nanoparticles during film assembly results in no enhancement, exhibiting an expected slightly greater blocking behavior (i.e., less current), in

fact, than the MUA SAM by itself (Figure 2). For additional verification that the current enhancement can be directly attributed to the presence of the CS-NPs, PLL-linked CS-NP films were washed repeatedly with a high concentration (0.25 M) KCl solution in order to disrupt the electrostatic interactions within the assembly and effectively desorb CS-NPs from the electrode (**Figure 3**).[50] Repeated washing of the films with high concentration salt solutions results in a steady decrease in the magnitude of the current enhancement and a definitive trend toward current responses typical for MUA SAM-modified electrodes.

The enhanced current achieved at the Au-NP film interface for the oxidation of H_2O_2 is clearly advantageous for electrochemical schemes where functionality depends on the efficiency of the modified electrode to detect small concentrations of H_2O_2 generated by enzymatic reactions. **Figure 4** illustrates the dramatic difference in sensitivity toward injected H_2O_2 for these films in terms of calibration curves. The oxidation of H_2O_2 at a MUA SAM modified electrode is clearly challenged, exhibiting sensitivity (slope) of only 0.25 μA/mM, whereas the PLL-linked CS-NP film assembly shows a sensitivity over 50x greater at 12.9 μA/mM, detecting H_2O_2 over a much lower range of concentrations. Indeed, the signal for 0.1 mM H_2O_2 at MUA SAMs is barely discernible, while even lower concentrations are not detectable above the background signal. In comparing the two film systems, the minimal detectable concentration of H_2O_2 is estimated to be ~790 μM for the MUA SAM compared to ~16 μM for the PLL-linked CS-NP film assembly (98% confidence).[51]

Factors Affecting Amperometric Response of PEM-NP Modified Electrodes

A number of experiments were specifically designed to identify film characteristics that affect the significant enhancement of the amperometric H_2O_2 signal at these Au-NP platforms. In

particular, experiments were designed to delineate the influence of several factors within the film, including Au-NP density, electronic coupling, permeability, and the type of Au-NP stabilizing ligand. The results of these experiments allow for a more optimal design of modified electrodes used for H_2O_2 detection.

The standard Au-NP film assembly, the platform showing significantly higher amperometric current response for the oxidation of H_2O_2, was constructed using three alternating exposures to PLL and CS-NPs solutions. Since the experimental evidence presented thus far suggests that the amperometric signal enhancement can be directly attributed to the CS-NPs presence within the film, the number of exposures to the PLL/CS-NP sequence was optimized with a series of experiments on increasingly thicker set of films, or increasing Au-NP density, and then compared to a MUA SAM control. The results of these experiments are summarized in **Figure 5**. Cyclic voltammetry tracking (Figure 5A) during the film assembly clearly indicates that with each exposure to the PLL/CS-NP sequence there is a corresponding increase in the charging current (capacitance), evidence that the CS-NPs are consistently incorporated into the film structure.[41] When tested for H_2O_2 response, however, the enhancement observed with these films did not correlate directly with the density of CS-NPs within the film (Figure 5B). A significant and increasing enhancement of amperometric current is observed for the first 3-4 exposures of the film to CS-NPs before plateauing for additional exposures. Thus, the electrode platform is optimized after 3-4 exposures to the CS-NPs. The dissipation of the current enhancement effect with additional exposures also suggests that the observed amperometric response is not necessarily a simple function of the Au-NP network being an extension of the working electrode's surface area. If these films were effectively extending the working electrode area out into solution, an idea also addressed in a later section (*vide infra*), one would not expect

11

the enhancement to curtail after only 3-4 exposures. Additionally, it is noteworthy to consider that the working electrode is first modified with a SAM of significant thickness that severely attenuates the current signal prior to any modification with the PEM-NP film (Figure 2). Since the MUA SAM remains intact as the film's anchoring underlayer throughout all subsequent measurements with Au-NP adlayers, a more complex mechanism must be responsible for the observed amperometric response.

A number of studies both in our laboratory and by others have been conducted that show that electronic communication (i.e., electronic coupling) within Au-NP composite films is a critical issue.[24-27] In this current study, both interfacial (i.e., NP film assembly-to-electrode) as well as inter-nanoparticle (i.e., NP-to-NP) electronic coupling were investigated to determine their effect on the amperometric response. Film geometries for these experiments were in accordance with those shown in **Scheme II**. For testing the importance of film-to-electrode electronic coupling, the amperometry of the standard film (Scheme I) was directly compared to a film assembly in which the CS-NPs were decoupled from the electrode via the addition of alternating polyelectrolyte layers of cationic PLL and anionic PSS inserted between the CS-NP density and the SAM-modified electrode (Scheme IIa). The comparison of amperometry for these films, displayed in **Figure 6**, shows that the intentional spacing of the CS-NP density from the electrode results in a dramatic decrease in the amperometric response toward H_2O_2. An even greater attenuation of the amperometric enhancement is observed if the same strategy of inserting PLL-PSS sequences as spacing layers is used to decouple the CS-NPs from each other and diminish inter-nanoparticle electronic communication (Scheme IIb). With diminished inter-nanoparticle electronic coupling, the film's amperometric sensitivity toward H_2O_2 closely resembles that of a MUA-SAM modified electrode (Figure 6) even though the film geometry

possesses CS-NP density very close to the electrode-film interface. These results suggest that both of these types of electronic coupling, both between the Au-NP film and the electrode and between the Au-NPs themselves, are important factors for these film assemblies to be optimized for the highly sensitive amperometric detection of H_2O_2.

As in any diffusional-based electrochemical experiment, the analyte's (i.e., H_2O_2) mass transport or access to the electrode interface can have a significant impact on the corresponding current response. For the present study, we have assessed access to the electrode in terms of permeability measurements,[52] where permeability index (PI) is defined as a ratio of amperometric current generated for 0.1 mM H_2O_2 at a modified electrode to that of a bare (unmodified) gold electrode (percentage). As expected, the modification of the bare gold with a MUA SAM results in a nearly completely blocked electrode interface and a corresponding PI of < 5% (Average: 2.0 $_{(\pm 1.1)}$%), with very little film-to-film variability. However, with the addition of the standard assembly of the PLL-linked CS-NP film (Scheme I), the current response is clearly restored, exhibiting a corresponding average PI of 96.6$_{(\pm 63.2)}$%, though with a noted high level of film-to-film variation. In fact, a significant number of experiments using electrodes with a PLL-linked CS-NP film modification showed permeability toward H_2O_2 that is equal to or greatly exceeds the permeability of a bare gold electrode. The collective permeability results suggest that, in addition to the other factors discussed, the ability of the PEM CS-NP film assembly to "extend" the working electrode out into solution while simultaneously behaving as if it is completely permeable toward H_2O_2 is important to its observed performance.[53] In other words, H_2O_2 molecules may be oxidized within the film at Au-NPs with the ET signal then transmitted to the transducer or working electrode via fast electron hopping mechanisms that have been noted for Au-NP films in other work.[41] Preliminary chronoamperometry experiments are supportive

(Supporting Information), yielding an apparent diffusion coefficients (D_{app}) at the MUA SAM and PLL-linked CS-NP interfaces that are three-fold smaller and one and half times greater, respectively, than the diffusion coefficient calculated for a bare gold electrode. Because the enhancement phenomenon seems independent of the presence or length of the SAM, electron tunneling through that portion of the film is not considered a major factor within these assemblies.

A critical component of understanding the signal enhancement provided by these Au-NP film assemblies may be related to the final factor explored in this study, the effect of the Au-NP's stabilizing ligands on the amperometric response. Noting the significant current enhancement observed at PLL-linked films with embedded CS-NPs (Figure 2), a variety of other types of ligand-protected nanoparticles were also embedded into PLL-linked films and tested for H_2O_2 to determine if this phenomenon was limited to CS-NPs. Citrate is a small, hydrophilic molecule featuring three carboxylic acid groups but does not covalently bond with the gold particle. NPs with a wide range of stabilizing ligands (**Scheme III**) were also successfully incorporated into PLL-linked film assemblies. More specifically, widely used and well-known NPs such as hexanethiolate (C6)/MUA MPCs (thiol-based protection),[41] cholate-stabilized NPs (steric bulk protection with some anionic properties)[49] and poly(N-vinyl-2-pyrrolidone) NPs (polymer-based protection)[45] were studied. The experimental details of these Au-NPs synthesis, characterization, and successful incorporation (i.e., spectroscopic/electrochemical tracking of film growth) into PLL-linked film assemblies are included within the Supporting Information. As shown in **Figure 7**, however, none of the films embedded with these different Au-NPs elicited an amperometric response toward H_2O_2 comparable to what is observed with the CS-NP film. In fact, the use of PLL-linked C6/MUA MPC films created with three different average

14

gold core diameters (see Supporting Information), resulted in a negligible response toward H_2O_2 (not shown) and were studied no further. Of these three alternative Au-NPs, only films embedded with PVP-NPs yielded significantly improved amperometric signal compared to the signal generated at a MUA SAM, though it provided only a quarter of the enhancement achieved with CS-NPs (Figure 7B). The observed higher response of PVP-NPs within PLL-linked films is interesting in that Schoenfisch et al. have reported PVP-doped aminosilane xerogels as a functional component of a glucose biosensing scheme that exhibit greater permeability and an enhanced amperometric response toward H_2O_2.[54] Our results suggest that the PVP coating of the Au-NPs may provide similar facilitation of H_2O_2 within these film assemblies.

Given the aforementioned results from Au-NPs with different protective ligands, it was hypothesized that the combination of thiol-based Au-NP protection with the underlying SAM at the electrode interface may be inhibiting the oxidation of H_2O_2 by creating an alkanethiolate barrier that prevents mass transfer of H_2O_2 to the Au-NP surface and/or introducing ET kinetic distance dependence. To test this hypothesis, Au-NPs were created with protective thiolated ligands of significantly smaller chainlengths (Scheme III) including highly stable thioctic acid-stabilized NPs (TAS-NPs) and 3-mercaptopropionic acid stabilized NPs (MPA-NPs). Both these ligands have carboxylic acid endgroups, though MPA-NPs possess a peripheral protective layer approximately half the chain length of the TAS-NPs which are very similar to hexane thiolate MPCs (Scheme III – dashed line, comparing structures a, b, and c). When tested with H_2O_2 injections (Figure 7), the typical response of the films incorporating TAS-NPs was actually less than at a MUA SAM. The response at films with embedded MPA-NPs, however, showed a rather substantial enhancement of H_2O_2 oxidation, though not as high as that of the original CS-NP films. It should be noted, however, that the MPA-NPs, with their thiol-based protection,

exhibited greater stability within the film, creating a trade-off between the greatest enhancement and stability compared with CS-NP films (Supporting Information).

Results from the different types of Au-NPs in these films, suggest that, in order to achieve a signal enhancement from the embedded Au-NPs, the peripheral skin of Au-NPs must be comprised of very short molecules or ligands, as is the case with CS-NPs and the MPA-NPs, both of which gave significantly enhanced amperometry. However, a final set of Au-NPs, capped with 4-mercaptobenzoic acid (MBA-NPs), was also embedded in PLL-linked films and tested. In this case, MBA represents a ligand that, while still thiol-based and carboxylated, has a greater effective "chain length" than the MPA but creates a film surrounding the Au-NPs where the ligand conjugation within that layer results in a more electronically conductive film compared to one of simple alkanethiolates of similar length (Scheme III – dashed line, comparing structures a, c, and d). The amperometric response toward H_2O_2 for PLL-linked films embedded with MBA-NPs showed a significant enhancement of current compared to a MUA SAM. This result suggests that, in order to achieve the enhancement effect, another important factor of the ligand protection may be the NP network's conductivity as a function of its peripheral ligand layer (aromatic vs. non-aromatic).

To illustrate a potential application of how one might benefit from the demonstrated signal enhancement provided by these Au-NP film assemblies at an electrode, a standard film of poly-L-lysine with embedded CS-NPs (Scheme I) was constructed at a bare region of a perfluoroalkoxy copolymer (Teflon) coated, small diameter, gold wire to create a modified "needle" electrode (Supporting Information).[55] While this aspect of the project will require refinement and development in future work, the preliminary results shown in the Supporting Information all suggest that a CS-NP/poly-L-lysine film is successful at significantly amplifying

the anodic signal from H_2O_2 oxidation upon injection. The results indicate that at a bare wire electrode, H_2O_2 is readily detected with a small current (e.g., ~0.3 nA) but is completely undetectable at a SAM-modified wire. Consistent with our prior findings in this study, assembly of the CS-NP/poly-L-lysine composite film at the same SAM on these wire electrode results in a significantly higher current signal (e.g., ~2.2 nA) compared to the bare wire. It is interesting to note that the wire electrode with the CS-NP film exhibits an increased capacitive or charging current after modification, suggesting that applications of such films to electrodes of this nature might naturally couple with electroanalytical techniques offering greater discrimination against background signals and faster data acquisition.[56] Functional, miniaturized electrodes such as these "needle" systems remain an important aspect of developing real-time or *in-vivo* 1st generation biosensors reliant on H_2O_2 detection.[55]

Conclusions

With this work, the inclusion of Au-NPs within thin film assemblies at electrodes has been shown as the basis of a highly sensitive transducer platform for 1st generation biosensing schemes. These Au-NP composite films are able to effectively enhance the amperometric signal of H_2O_2 making this study an important part of the growing body of work dedicated to NP-based amplification for biosensing.[57] In particular, while the current study shows CS-NP embedded PLL films to be particularly sensitive to H_2O_2 detection, it also specifically identifies the following factors to consider when designing these platforms: (1) the benefit and limitation of the film's Au-NP density; (2) the importance of electronic coupling both among Au-NPs (interparticle) as well as between the film assembly and the electrode itself; (3) access of the analyte, in this case, H_2O_2, to the electrode/Au-NPs within the film and; (4) the critical implications of the type of

protective layer on the embedded Au-NPs. With regard to this latter aspect of the films, it appears that in order to have enhanced amperometric signals, NP protective layers need to be composed of small, carboxylated molecules whose conductivity within a film may be enhanced aromaticity (conjugation). While thiol-based protection of the Au-NPs such as MPA-NPs and MBA-NPs provide greater degrees of stability compared to CS-NPs, the chain length of the alkanethiols ligands incorporated for NP protection must be sufficiently short enough to not introduce detrimental distance dependence of ET or inadvertently introduce a mass transfer barrier for H_2O_2.

Having established these highly sensitive Au-NP interfaces for efficient H_2O_2 detection, future work on these materials will involve the study of their performance when enzymatic reactions are the source of H_2O_2. That is, the PLL-linked NP film assemblies developed here may be integrated as part of more complete biosensing strategies involving enzyme-doped sol-gels, for example, and subsequent biocompatible coatings such as polyurethane membranes that add selectivity and improve the signal-to-noise ratios of the NP interfaces (Supporting Information).[52, 54] To this end, the presented findings highlight several important parameters for consideration when designing biosensors with critical NPs functionality.

Acknowledgements

Supporting Information Available:

TEM and spectroscopy characterization of CS-NPs as well as electrochemical probing of potassium ferricyanide at stages of PLL-linked CS-NP film assemblies; Amperometric *I-T* curves and permeability studies for H_2O_2 injections at PLL-linked CS-NP or TAS-NP film assemblies at MHA and MHDA SAMs. Synthetic details for various Au-NPs, including TAS-NPs, MPCs, MPA-NPs, CHO-NPs, PVP-NPs, and MBA-NPs. Preliminary findings of signal enhancement at wire electrodes modified with CS-NP film assemblies. This information is available free of charge via the Internet at http://pubs.acs.org/.

References

(1) Chang, M. L.; Dong, H.; Cao, X.; Luong, J. H. T.; Zhang, X. Implantable Electrochemical Sensors for Biomedical and Clinical Applications: Progress, Problems, and Future Possibilities. *Curr. Med. Chem.* **2007**, *14*, 937-951.

(2) Kotanen, C. N.; Moussy, F. G.; Carrara, S.; Guiseppi-Elie, A. Implantable Enzyme Amperometric Biosensors. *Biosens. Bioelectron.* **2012**, *35*, 14.

(3) Wang, J. Electrochemical Glucose Biosensors. *Chem. Rev.* **2008**, *108*, 814-825.

(4) Villalonga, R.; Díez, P.; Yáñez-Sedeño, P.; Pingarrón, J. M. Wiring Horseradish Peroxidase on Gold Nanoparticles-Based Nanostructured Polymeric Network for the Construction of Mediatorless Hydrogen Peroxide Biosensor. *Electrochim. Acta* **2011**, *56*, 4672-4677.

(5) Ciobanu, M.; Taylor, D. E., Jr.; Wilburn, J. P.; Cliffel, D. E. Glucose and Lactate Biosensors for Scanning Electrochemical Microscopy Imaging of Single Live Cells. *Anal. Chem.* **2008**, *80*, 2717-2727.

(6) Chandra, D.; Jena, B. K.; Raj, C. R.; Bhaumik, A. Functionalized Mesoporous Cross-Linked Polymer as Efficient Host for Loading Gold Nanoparticles and its Electrocatalytic Behavior for Reduction of H2O2. *Chem. Mater.* **2007**, *19*, 6290-6296.

(7) Gamero, M.; Pariente, F.; Lorenzo, E.; Alonso, C. Nanostructured Rough Gold Electrodes for the Development of Lactate Oxidase-Based Biosensors. *Biosens. Bioelectron.* **2010**, *25*, 2038-2044.

(8) Walcarius, A.; Collinson, M. M. Analytical Chemistry with Silica Sol-Gels: Traditional Routes to New Materials for Chemical Analysis. *Annu. Rev. Anal. Chem.* **2009**, *2*, 121-143.

(9) Gupta, R. Bioactive Materials for Biomedical Applications using sol–gel Technology. *Biomed. Mater. (Bristol, U.K.)* **2008**, *3*, 034005; ARTN 034005.

(10) Pauliukaite, R. Development of Electrochemical Biosensors Based on Sol-Gel Enzyme Encapsulation and Protective Polymer Membranes. *Anal. Bioanal. Chem.* **2008**, *390*, 1121-1131.

(11) Guo, S.; Dong, S. Biomolecule-Nanoparticle Hybrids for Electrochemical Biosensors. *TrAC, Trends Anal. Chem.* **2009**, *28*, 96-109.

(12) Kerman, K.; Saito, M.; Tamiya, E.; Yamamura, S.; Takamura, Y. Nanomaterial-Based Electrochemical Biosensors for Medical Applications. *TrAC, Trends Anal. Chem.* **2008**, *27*, 585-592.

(13) Pandey, P.; Datta, M.; Malhotra, B. D. Prospects of Nanomaterials in Biosensors. *Anal. Lett.* **2008**, *41*, 159-209.

(14) Escosura-Muniz, d. l. A.; Ambrosi, A.; Merkoci, A. Electrochemical Analysis with Nanoparticle-Based Biosystems. *TrAC, Trends Anal. Chem.* **2008**, *27*, 568.

(15) Siangproh, W.; Dungchai, W.; Rattanarat, P.; Chailapakul, O. Nanoparticle-Based Electrochemical Detection in Conventional and Miniaturized Systems and their Bioanalytical Applications: A Review. *Anal. Chim. Acta* **2011**, *690*, 10-25.

(16) Wang, F. Electrochemical Sensors Based on Metal and Semiconductor Nanoparticles. *Mikrochim. Acta* **2009**, *165*, 1-22.

(17) Pingarrón, J. M.; Yáñez-Sedeño, P.; González-Cortés, A. Gold Nanoparticle-Based Electrochemical Biosensors. *Electrochim. Acta* **2008**, *53*, 5848-5866.

(18) Liu, S.; Leech, D.; Ju, H. Application of Colloidal Gold in Protein Immobilization, Electron Transfer, and Biosensing. *Anal. Lett.* **2003**, *36*, 1-19.

(19) Guo, S.; Wang, E. Synthesis and Electrochemical Applications of Gold Nanoparticles. *Anal. Chim. Acta* **2007**, *598*, 181.

(20) Zhao, J.; Henkens, R. W.; Stonehuerner, J.; O'Daly, J. P.; Crumbliss, A. L. Direct Electron Transfer at Horseradish Peroxidase-Colloidial Gold Modified Electrodes. *J. Electroanal. Chem.* **1992**, *327*, 109-119.

(21) Niemeyer, M. Nanoparticles, Proteins, and Nucleic Acids: Biotechnology Meets Materials Science. *Angew Chem. Int. Ed. Engl.* **2001**, *40*, 4128-4158.

(22) Shenhar, R.; Rotello, V. M. Nanoparticles: Scaffolds and Building Blocks. *Acc. Chem. Res.* **2003**, *36*, 549-561.

(23) Hicks, J. F.; Seok-Shon, Y.; Murray, R. W. Layer-by-Layer Growth of Polymer/Nanoparticle Films Containing Monolayer-Protected Gold Clusters. *Langmuir* **2002**, *18*, 2288-2294.

(24) Bradbury, C. R.; Zhao, J.; Fermin, D. J. Distance-Independent Charge-Transfer Resistance at Gold Electrodes Modified by Thiol Monolayers and Metal Nanoparticles. *J. Phys. Chem. C* **2008**, *112*, 10153-10160.

(25) Zhao, J.; Bradbury, C. R.; Huclova, S.; Potapova, I.; Carrara, M.; Fermin, D. J. Nanoparticle-Mediated Electron Transfer Across Ultrathin Self-Assembled Films. *J. Phys. Chem. B* **2005**, *109*, 22985-22994.

(26) Dowdy, C. E.; Leopold, M. C. Enhanced Electrochemistry of Nanoparticle-Embedded Polyelectrolyte Films: Interfacial Electronic Coupling and Distance Dependence. *Thin Solid Films* **2010**, *519*, 790-796.

(27) Doan, T.; Day, R.; Leopold, M. Optical and Electrochemical Properties of Multi-Layer Polyelectrolyte Thin Films Incorporating Spherical, Gold Colloid Nanomaterials. *J. Mater. Sci.* **2012**, *47*, 108-120.

(28) Galyean, A. A.; Day, R. W.; Malinowski, J.; Kittredge, K. W.; Leopold, M. C. Polyelectrolyte-Linked Film Assemblies of Nanoparticles and Nanoshells: Growth, Stability, and Optical Properties. *J. Colloid Interface Sci.* **2009**, *331*, 532-542.

(29) Russell, L. E.; Galyean, A. A.; Notte, S. M.; Leopold, M. C. Stable Aqueous Nanoparticle Film Assemblies with Covalent and Charged Polymer Linking Networks. *Langmuir* **2007**, *23*, 7466.

(30) Kumar, S.; Kwak, K.; Lee, D. Amperometric Sensing Based on Glutathione Protected Au25 Nanoparticles and their pH Dependent Electrocatalytic Activity. *Electroanalysis* **2011**, *23*, 2116-2124.

(31) Kannan, P.; Chen, H. L.; Lee, V. T.; Kim, D. Highly Sensitive Amperometric Detection of Bilirubin using Enzyme and Gold Nanoparticles on Sol-Gel Film Modified Electrode. *Talanta* **2011**, *86*, 400.

(32) Hsiao, Y.; Su, W.; Cheng, J.; Cheng, S. Electrochemical Determination of Cysteine Based on Conducting polymers/gold Nanoparticles Hybrid Nanocomposites. *Electrochim. Acta* **2011**, *56*, 6887.

(33) Lei, C. X.; Wang, H.; Shen, G.; Yu, R. Q. Immobilization of Enzymes on the Nano-Au Film Modified Glassy Carbon Electrode for the Determination of Hydrogen Peroxide and Glucose. *Electroanalysis* **2004**, *16*, 736.

(34) Yagati, A. K.; Lee, T.; Min, J.; Choi, J. Electrochemical Performance of Gold nanoparticle–cytochrome c Hybrid Interface for H2O2 Detection. *Colloids Surf., B: Biointerfaces* **2012**, *92*, 161-167.

(35) Zhang, B.; Cui, Y.; Chen, H.; Liu, B.; Chen, G.; Tang, D. A New Electrochemical Biosensor for Determination of Hydrogen Peroxide in Food Based on Well-Dispersive Gold Nanoparticles on Graphene Oxide. *Electroanalysis* **2011**, *23*, 1821.

(36) Gao, F.; Yuan, R.; Chai, Y.; Chen, S.; Cao, S.; Tang, M. Amperometric Hydrogen Peroxide Biosensor Based on the Immobilization of HRP on Nano-Au/Thi/poly (*p*-Aminobenzene Sulfonic Acid)-Modified Glassy Carbon Electrode. *J. Biochem. Biophys. Methods* **2007**, *70*, 407.

(37) Baccar, H.; Ktari, T.; Abdelghani, A. Functionalized Palladium Nanoparticles for Hydrogen Peroxide Biosensor. *Int. J. Electrochem.* **2011**, *6*, 4.

(38) Dominguez, E.; Guillaume, S.; Arantzazu, N. Electrostatic Assemblies for Bioelectrocatalytic and Bioelectronic Applications. *Electroanalysis* **2006**, *18*, 1871-1878.

(39) Musick, M. D.; Keating, C. D.; Lyon, L. A.; Botsko, S. L.; Pena, D. J.; Holliway, W. D.; McEvoy, T. M.; Richardson, J. N.; Natan, M. J. Metal Films Prepared by Stepwise Assembly. 2. Construction and Characterization of Colloidal Au and Ag Multilayers. *Chem. Mater.* **2000**, *12*, 2869-2881.

(40) Bradbury, C. R.; Zhao, J.; Fermin, D. J. Distance-Independent Charge-Transfer Resistance at Gold Electrodes Modified by Thiol Monolayers and Metal Nanoparticles. *J. Phys. Chem. C* **2008**, *112*, 10153-10160.

(41) Loftus, A. F.; Reighard, K. P.; Kapourales, S. A.; Leopold, M. C. Monolayer-Protected Nanoparticle Film Assemblies as Platforms for Controlling Interfacial and Adsorption Properties in Protein Monolayer Electrochemistry. *J. Am. Chem. Soc.* **2008**, *130*, 1649-1661.

(42) Lin, S.; Tsai, Y.; Chen, C.; Lin, C.; Chen, C. Two-Step Functionalization of Neutral and Positively Charged Thiols Onto Citrate-Stabilized Au Nanoparticles. *J. Phys. Chem. B* **2004**, *108*, 2134-2139.

(43) Gao, J.; Huang, X.; Liu, H.; Zan, F.; Ren, J. Colloidal Stability of Gold Nanoparticles Modified with Thiol Compounds: Bioconjugation and Application in Cancer Cell Imaging. *Langmuir* **2012**, *28*, 4464.

(44) Gies, A. P.; Hercules, D. M.; Cliffel, D. E. Electrospray Mass Spectrometry Study of Tiopronin Monolayer-Protected Gold Nanoclusters. *J. Am. Chem. Soc.* **2007**, *129*, 1095.

(45) Sun, Y.; Mayers, B. T.; Xia, Y. Template-Engaged Replacement Reaction: A One-Step Approach to the Large-Scale Synthesis of Metal Nanostructures with Hollow Interiors. *Nano. Lett.* **2002**, *2*, 481-485.

(46) Silvert, P.; Herrera-Urbina, R.; Duvauchelle, N.; Vijayakrishnan, V.; Tekaia-Elhsissen, K. Preparation of Colloidal Silver Dispersions by the Polyol Process: Part 1 - Synthesis and Characterization. *J. Mater. Chem.* **1996**, *6*, 573-577.

(47) Han, M. Y.; Quek, C. H.; Huang, W.; Chew, C. H.; Gan, L. M. A Simple and Effective Chemical Route for the Preparation of Uniform Nonaqueous Gold Colloids. *Chem. Mater.* **1999**, *11*, 1144-1147.

(48) Levi-Kalisman, Y.; Jadzinsky, P. D.; Kalisman, N.; Tsunoyama, H.; Tsukuda, T.; Bushnell, D. A.; Kornberg, R. D. Synthesis and Characterization of $Au_{102}(p\text{-}MBA)_{44}$ Nanoparticles. *J. Am. Chem. Soc.* **2011**, *133*, 2976.

(49) Qiao, Y.; Chen, H.; Lin, Y.; Huang, J. Controllable Synthesis of Water-Soluble Gold Nanoparticles and their Applications in Electrocatalysis and Surface-Enhanced Raman Scattering. *Langmuir* **2011**, *27*, 11090-11097.

(50) Doan, T. T.; Vargo, M. L.; Gerig, J. K.; Gulka, C. P.; Trawick, M. L.; Dattelbaum, J. D.; Leopold, M. C. Electrochemical Analysis of Azurin Thermodynamic and Adsorption

Properties at Monolayer-Protected Cluster Film Assemblies: Evidence for a More Homogeneous Adsorption Interface. *J. Colloid Interface Sci*. **2010**, *352*, 50-58.

(51) Harris, D.C. Quantitative Chemical Analysis, 6ᵗʰ Ed. W.H. Freeman and Company, New York, 2003.

(52) Koh, A.; Riccio, D. A.; Sun, B.; Carpenter, A. W.; Nichols, S. P.; Schoenfisch, M. H. Fabrication of Nitric Oxide-Releasing Polyurethane Glucose Sensor Membranes. *Biosens. Bioelectron*. **2011**, *28*, 17-24.

(53) Stroe-Biezen, S. v.; Everaerts, F. M.; Janssen, L. J. J.; Tacken, R. A. Diffusion Coefficients of Oxygen, Hydrogen Peroxide and Glucose in a Hydrogel. *Anal. Chim. Acta* **1993**, *273*, 553.

(54) Schoenfisch, M. H.; Rothrock, A. R.; Shin, J. H.; Polizzi, M. A.; Brinkley, M. F.; Dobmeier, K. P. Poly(Vinylpyrrolidone)-Doped Nitric Oxide-Releasing Xerogels as Glucose Biosensor Membranes. *Biosens. Bioelectron*. **2006**, *22*, 306-312.

(55) Yan, Q.; Major, T. C.; Bartlett, R. H.; Meyerhoff, M. E. Intravascular glucose/lactate sensors prepared with nitric oxide releasing poly(lactide-co-glycolide)-based coatings for enhanced biocompatibility. *Biosens. Bioelectron*. **2011**, *26*, 4276-4282.

(56) Campell-Rance, D.; Doan, T.; Leopold, M. Sweep, Step, Pulse, and Frequency-Based Techiques Applied to Protein Monolayer Electrochemistry at Nanoparticle Interfaces. *J. Electroanal. Chem*. **2011**, *665*, 343-354.

(57) Cao, X.; Ye, Y.; Liu, S. Gold Nanoparticle-Based Signal Amplification for Biosensing. *Anal. Biochem*. **2011**, *417*, 1.

Scheme I

NP
PLL
NP
PLL
NP
PLL
MUA
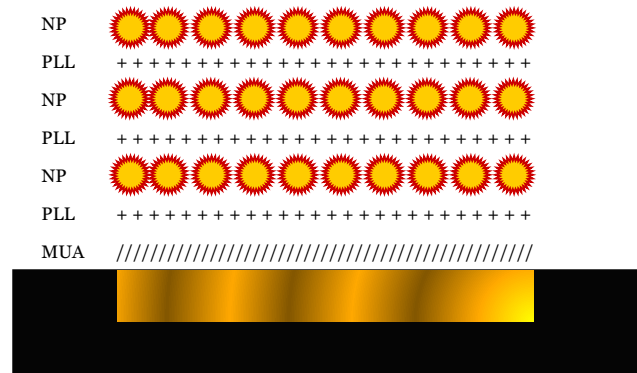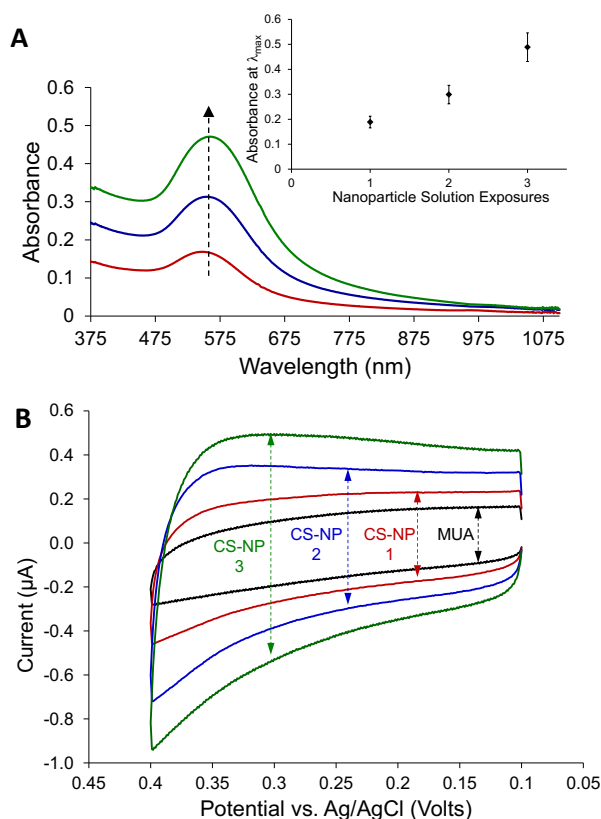
Figure 1. Examples of tracking methods for gold nanoparticle (Au-NP) film assembly and incorporation of NPs. **(A)** Typical UV-Vis spectra of poly-L-lysine (PLL) linked TAS-NP films during assembly procedure with distinctive Au-NP absorbance increasing (black arrow) after each exposure to Au-NP solution. **Inset:** Absorbance at λ_{max} tracked over three exposures to the TAS-NP solution during film assembly. **(B)** Cyclic voltammetry of PLL-linked CS-NP film assemblies showing typical increasing double-layer capacitance with increasing exposures and incorporation of CS-NPs into film assembly. Voltammetry was recorded at 100 mV/sec in 4.4 mM potassium phosphate buffer (pH = 7).
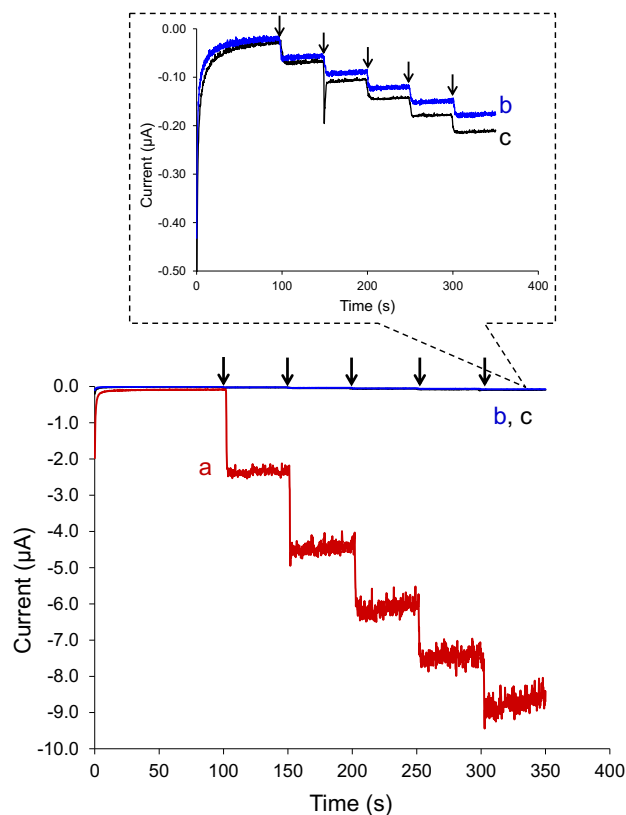
Figure 2. Representative amperometric *I-t* curves during H_2O_2 injections (black arrows) to a solution containing gold electrodes modified with (a) PLL-linked CS-NP film assembly at a MUA SAM; (b) polyelectrolyte multilayer (PEM) film of alternating layers of PLL and PSS (substituted for NPs) at a MUA SAM; and (c) a MUA SAM. Each 10 μL injection (black arrows) of 0.25 M H_2O_2 results in a 0.1 mM H_2O_2 increase of the stirred 4.4 mM phosphate buffer (pH=7) bulk solution.
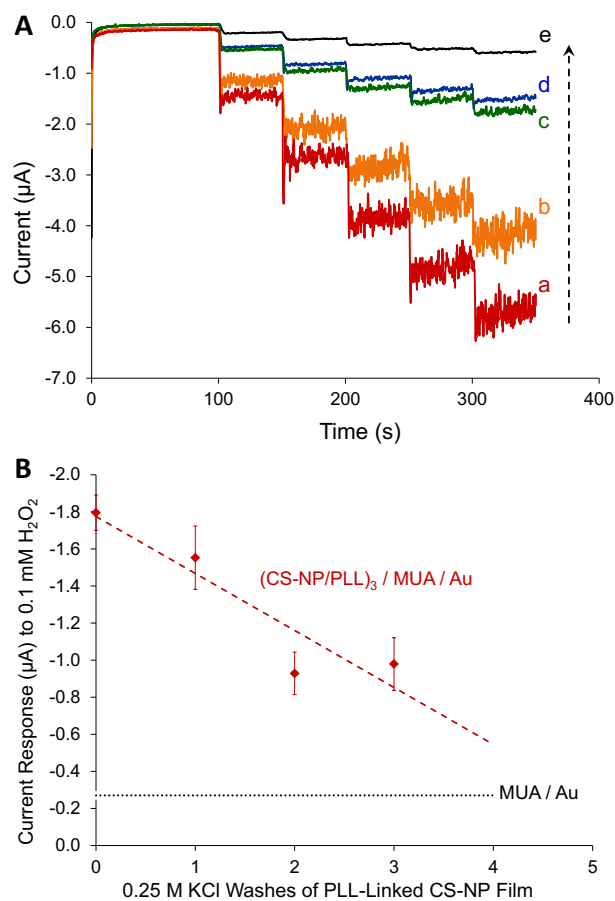
Figure 3. **(A)** Amperometric *I-t* curves of sequential H_2O_2 injections at a PLL-linked CS-NP film after exposure to successive washes (a-d) of 0.25 M KCl to systematically remove the CS-NPs and compared to corresponding response at a MUA SAM modified electrode (e). **(B)** Current response to 0.1 mM H_2O_2 (first step) at a Au / MUA / (CS-NP/PLL)$_3$ versus a Au / MUA SAM interface.
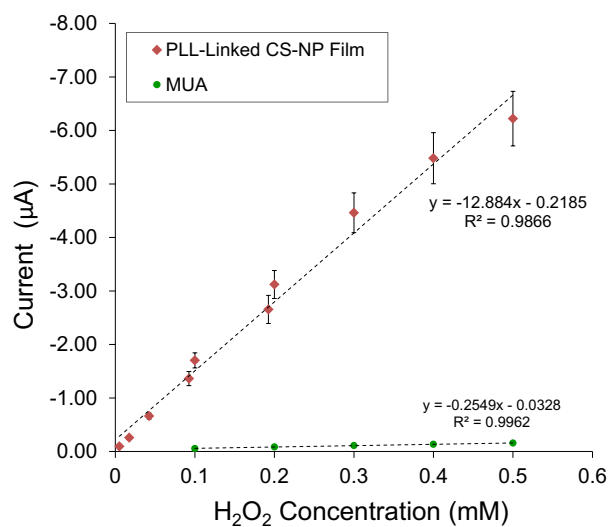
Figure 4. Calibration curves for amperometric response to increasing H_2O_2 concentrations for PLL-linked CS-NP films versus a MUA SAM modified electrode. Note: In some cases standard error bars are smaller than the markers.
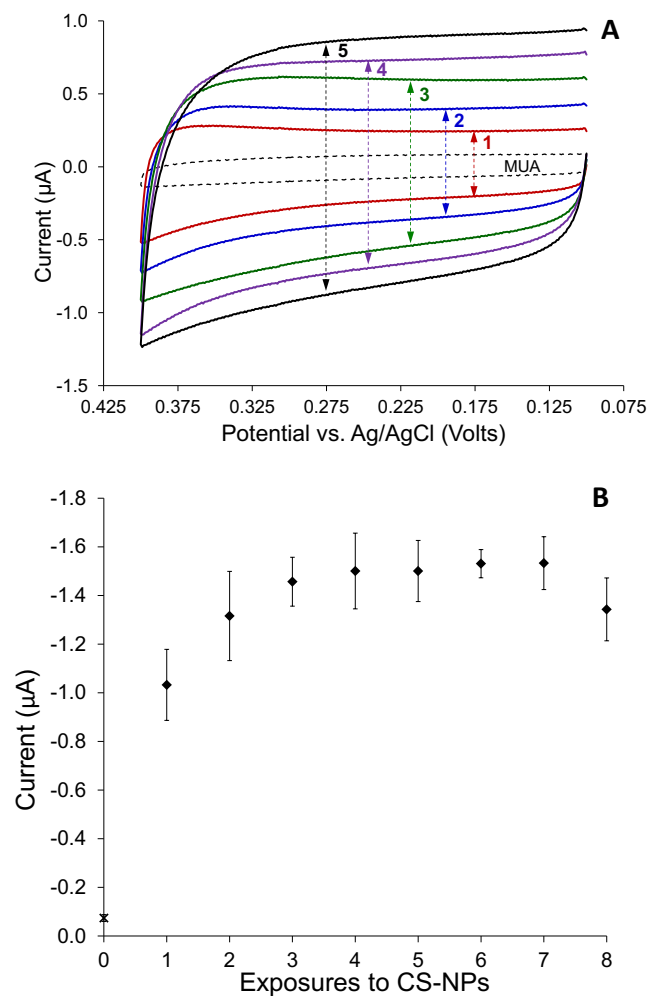
Figure 5. **(A)** Cyclic voltammetry showing the increasing capacitance of the film assembly during first five exposures of a MUA SAM to alternating solutions poly-L-lysine (PLL) and CS-NPs. **(B)** Enhanced current response of PLL-linked CS-NP films with varying exposures to CS-NPs toward injection of 0.1 mM H_2O_2. Note: Current response for 0 exposures to CS-NPs (x) is for the MUA SAM without any CS-NPs. Voltammetry was recorded at 100 mV/sec in 4.4 mM potassium phosphate buffer (pH = 7).

Scheme II

a

NP	
PLL	+ +
NP	
PLL	+ +
NP	
PLL	+ +
PSS	- -
PLL	+ +	} x 10
MUA	///
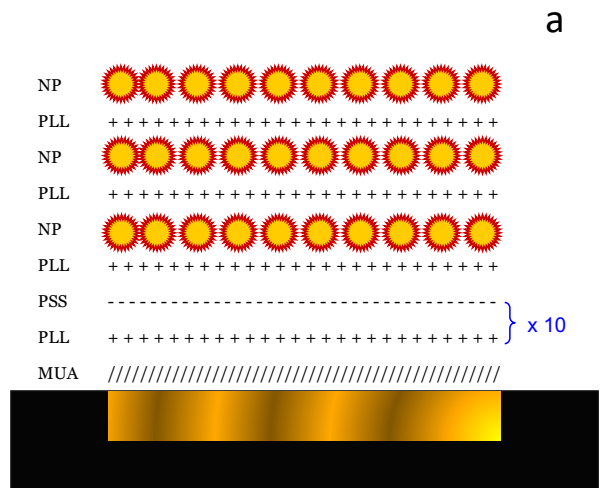
Nanoparticle film-electrode coupling

b

NP	
PLL	+ +
PSS	- -
PLL	+ +	} x 10
NP	
PLL	+ +
PSS	- -
PLL	+ +	} x 10
NP	
PLL	+ +
MUA	///
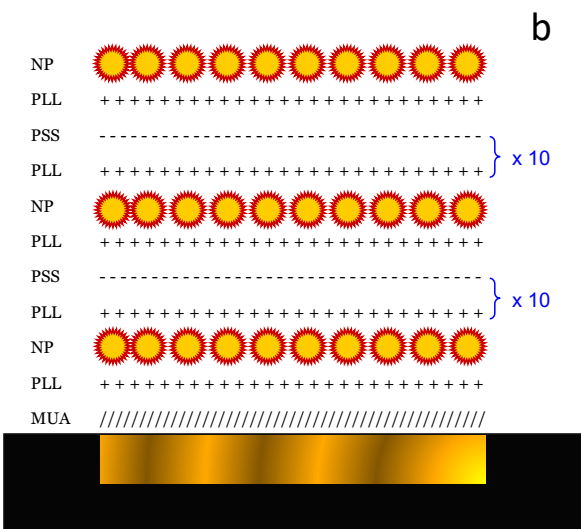
Inter-nanoparticle coupling

31
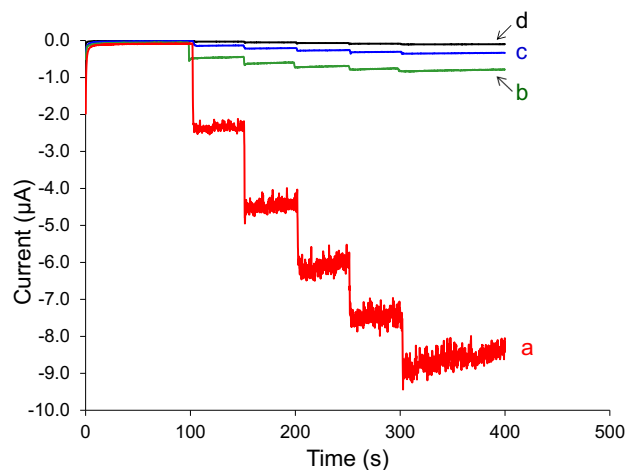
Figure 6. Amperometric *I-t* curves of sequential H_2O_2 injections at (a) a standard PLL-linked CS-NP film (Scheme I); (b) a PLL-linked CS-NP film with increased electrode-nanoparticle spacing using alternating PLL/PSS (10x) sequences that electronically decouple the working electrode from the NPs (Scheme II-a); (c) a PLL-linked CS-NP film with increased nanoparticle-nanoparticle spacing using alternating PLL/PSS (10x) sequences that electronically decouple inter-nanoparticle electronic interactions (Scheme II-b); (d) a MUA SAM.

Scheme III

a-MPC
(C6/MUA)
b-TA
c-MPA
d-MBA
e-CHO
f-PVP
g-Citrate
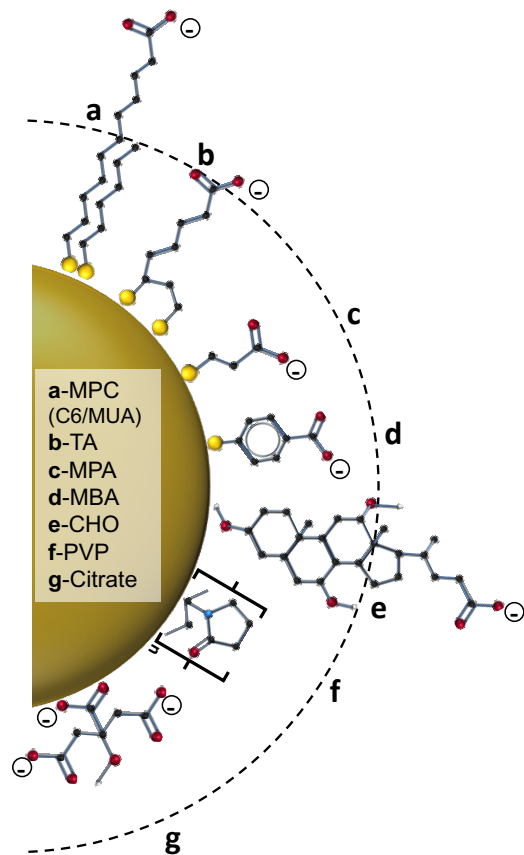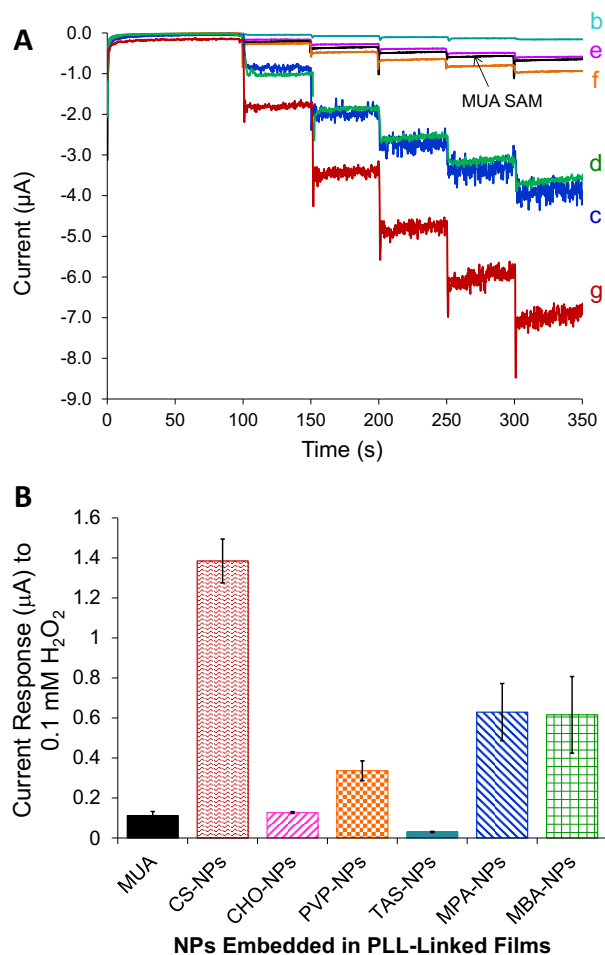
Figure 7. (A) Representative amperometric *I-t* curves during H_2O_2 injections (50 sec. intervals) to a solution containing gold electrodes modified with different types of PLL-linked Au-NPs featuring various ligand protections. Films assembled with CS-NPs, MPA-NPs, and MBA-NPs **(c,d,g)** all resulted in enhanced current responses to H_2O_2 while films embedded with TAS-NPs, CHO-NPs, and PVP-NPs **(b,e,f)** showed very little or no significant enhancement of the signal. *Note:* Au-NP ligand designations (b-g) are as shown in Scheme III; **(B)** Quantitative comparison of current response at different PLL-linked NP film assemblies toward 1st injection of H_2O_2 (0.1 mM). All responses are compared to that of a MUA SAM and each 10 μL injection (black arrows) of 0.25 M H_2O_2 results in a 0.1 mM H_2O_2 increase of the stirred 4.4 mM phosphate buffer (pH=7) bulk solution.

Graphical Abstract (4 x 8 cm)